



Nanoalumina Synthesized from *Solanum torvum* Leaves: A Green Approach

P. PANDIAN¹, A. KASTHURI², P. SAMEERABANU³ and K. K. ILAVENIL^{4*}

¹Department of Chemistry, Thanthai Periyar Government Arts and Science College (Autonomous), Affiliated to Bharathidasan University, Tiruchirappalli-620 023, Tamilnadu, India.

²Department of Chemistry, Nehru Memorial College (Autonomous), Affiliated to Bharathidasan University, Puthanampatti-621 007, Tiruchirappalli, Tamilnadu, India.

³Department of Mathematics, School of Engineering and Technology, Dhanalakshmi Srinivasan University, Samayapuram, Tiruchirappalli-621 112, Tamilnadu, India.

⁴Department of Chemistry, School of Engineering and Technology, Dhanalakshmi Srinivasan University, Samayapuram, Tiruchirappalli-621 112, Tamilnadu, India.

*Corresponding author E-mail: ilavenilkk.set@dsuniversity.ac.in

<http://dx.doi.org/10.13005/ojc/400510>

(Received: April 19, 2024; Accepted: September 24, 2024)

ABSTRACT

This study investigates the eco-friendly synthesis of aluminum oxide nanoparticles (Al_2O_3 NPs) using *Solanum torvum* leaf extract, highlighting its potential in sustainable nanotechnology. The synthesized nanoparticles, with an average size of 94.6nm, exhibited high crystallinity and diverse morphologies as confirmed through Scanning Electron Microscopy and X-ray crystallography. The antibacterial properties of these Al_2O_3 NPs were evaluated against a range of pathogens, including *Escherichia coli* and *Candida albicans*, where significant inhibition zones were observed. The findings underscore the effectiveness of *Solanum torvum* leaf extract as a green synthesis medium for producing Al_2O_3 nanoparticles. With their promising antibacterial activity, these nanoparticles hold potential for application in various fields, from healthcare to environmental protection, contributing to the development of environmentally friendly and sustainable nanomaterials.

Keywords: Aluminium oxide nanoparticles, *Solanum torvum*, Characterization, Scanning Electron Microscope, Pathogens, *Escherichia coli*.

INTRODUCTION

Green synthesis employs plant extracts from roots, stems, leaves, flowers, and seeds. Flavonoids, alkaloids, phenolics, and others are found in the extracts. Plant extract with metal salts produce nanoparticles of varied sizes,

shapes, and surfaces. Because they renew and are nonpathogenic, leaves are the major source of metabolites. Extracts derived from seeds, bark, flowers, tubers, and roots have the ability to synthesize nanoparticles, including metal oxide nanoparticles. Phytochemicals within these plant materials facilitate the degradation of metal ions,



resulting in the formation of metal nanoparticles. Amino acids diminish metal oxide. Oxygen degrades metal ions. Electrostatic attraction agglomerates phytochemicals and metal oxide¹. Plant phenolic compounds possessing carboxyl and hydroxyl groups are known to inhibit superoxide. Additionally, proteins extracted from plant material are capable of synthesizing metal nanoparticles through the utilization of both high- and low-weight phytochemicals, proteins, and starch^{2,3}. Researchers have tried to apply nanotechnology to everything in recent years. Nanoparticles physicochemical properties affect their antibacterial activity, and we know they differ from bulk particles⁴.

Leaf extracts from diverse plant species contain phytochemicals such as flavonoids, alkaloids, and phenols that can reduce and stabilise nanoparticle formation. These phytochemicals reduce metal ions to nanoparticles. Plant extract nanoparticle production is cheaper, non-toxic, and eco-friendly. Antibacterial, antifungal, and anticancer nanoparticles from leaf extracts have been studied. Nanoparticles have at least one dimension under 100nm. Their unusual physical and chemical features make them appealing for application in medicine, electronics, and energy.

20% of the worldwide nanoparticle market is Al_2O_3 NPs, which may be utilised in coating, textile functionalization, medication delivery, and vaccines to alter the immune response and increase human immunisation. Al_2O_3 NPs can disrupt biological systems and produce catastrophic toxicological consequences, according to earlier studies⁵. Aluminium oxide nanoparticles have features that are valuable in electronics, catalysis, and biomedical engineering. They have better mechanical, electrical, and thermal characteristics due to their small dimensions and high surface area to volume ratio. Surface changes can also adapt nanoparticle characteristics to specific applications. Aluminium oxide nanoparticles, like other nanoparticles, can permeate biological tissues and pose health and environmental hazards due to their tiny size. These metal NPs will be released into the biological system at tremendous rates, exposing living organisms to them. Al_2O_3 and Ag metal NPs have been linked to reproductive

system toxicity. Al_2O_3 NPs, comprising 20% of the global market, are used in coatings, textiles, medications, and vaccines to enhance immune responses and immunization⁶⁻⁹.

Industries, particularly in medicine, employ inorganic nanoparticles like silver, copper, aluminum, and platinum oxides due to their stable nature and uniform nanoparticle production. Physicochemical processes create industrial nanoparticles. These methods involve harmful substances that harm people and the environment¹. Researchers are evaluating metal and metal oxide nanoparticles optical, electrical, magnetic, and catalytic properties to validate their novel production method¹⁰.

Plant extracts provide several benefits over chemical approaches for synthesising Al_2O_3 NPs, including cheap cost, eco-friendliness, and the capacity to generate nanoparticles with controllable size and form. Plant extracts contain phytochemicals such as phenolic compounds, flavonoids, and terpenoids that can reduce and stabilise Al_2O_3 NPs. By reducing metal ions in solution, these phytochemicals can create nanoparticles. Plant extract-derived Al_2O_3 NPs have large surface area, biocompatibility, and excellent antibacterial and antifungal activity. Drug delivery, biosensors, and wastewater treatment are further possible uses. Al_2O_3 NPs synthesised from plant extracts are biocompatible and low-toxic, making them intriguing candidates for drug administration, imaging, and tissue engineering. They are effective antibacterial and antifungal agents that may be used in water treatment, water purification, pollution abatement, solar cells, LEDs, food preservation, and wound healing¹¹⁻¹⁷.

Solanum torvum

Solanum torvum, commonly known as turkey berry, is a small thorny shrub widely found in tropical regions. Traditionally, its fruits and leaves have been used in folk medicine for treating infections, inflammation, and hypertension. The plant is rich in phytochemicals such as alkaloids, flavonoids, tannins, saponins, and steroids, which contribute to its antibacterial, antioxidant, and antifungal properties. These compounds make *Solanum torvum* valuable in medicinal applications, aiding in the treatment of ailments

like diabetes, digestive disorders, and respiratory infections. Recently, the plant has gained attention for its role in green chemistry, particularly in synthesizing eco-friendly nanoparticles, such as aluminum oxide, for biomedical and environmental uses. Its phytochemicals act as reducing and stabilizing agents, making it a sustainable resource in nanotechnology. Many researchers have synthesised nanoparticles like zinc oxide¹⁸, silver nanoparticles.^{19,20}

MATERIALS AND METHODS

Preparation of leaf extracts

The *Solanum torvum* leaves, free from any insect or fungal attack were gathered. The leaves were washed with NaOCl (1%) and then by double distilled water to remove earthy impurities. After washing, plant material was sun-dried or dehydrated for a week. Preventing mould and maintaining plant active chemicals required this

procedure. The dried leaves were powdered and sieved.

Green synthesis of Aluminium oxide nanoparticles

A beaker containing 20 g of powdered *Solanum torvum* leaf was placed on a hot plate, and 100 millilitres of doubly distilled water was poured to it (Fig. 1). The mixture was agitated for thirty minutes. After collecting the plant extract, it was processed by filtration and centrifugation. After combining the plant extract with 100 mL of 10 mmol aluminium nitrate solution for one hour, the mixture was analysed. While stirring, 100 mL of sodium hydroxide with a concentration of 0.1 M was added in stages. Because of the presence of nanoparticles of aluminium oxide, the liquid became cloudy, and the previously colourless substance took on a brown shade. Throughout the synthesis, sterile conditions were maintained, and clean glassware and equipment were utilised. This was done to prevent contamination²¹⁻²⁴.

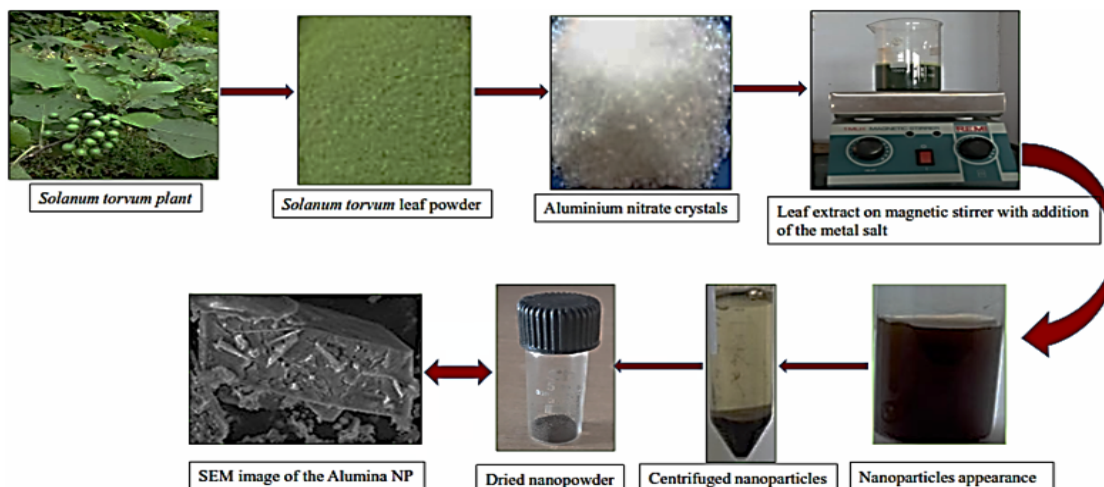


Fig. 1. Synthesis of Alumina nanoparticles

RESULTS AND DISCUSSION

Spectroscopy of Alumina NPs

The UV absorption peak (Fig. 2) of Al_2O_3 nanoparticles at 268nm indicates that these particles have a high degree of crystallinity. This is because the peak is associated with the electronic transitions of the aluminium oxide bonds in the nanoparticle structure. Specifically, the peak at 268nm corresponds to the $\pi-\pi^*$ transition of the surface-bound oxygen vacancies in Al_2O_3 ²⁵.

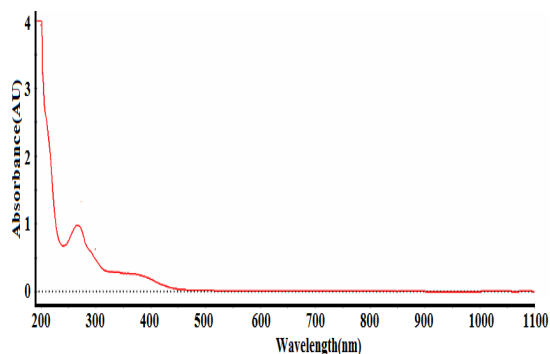


Fig. 2. UV Spectrum of Alumina NPs

The existence of O-H stretching vibrations of hydroxyl groups in the organic molecules (Fig. 3) that are present in the leaf extract is most likely the cause of the peak that can be found at 3270.01 cm^{-1} . It is possible that the stretching vibrations of CN groups are responsible for the peak that may be found at 2360.08 cm^{-1} . It's possible that the existence of C=O stretching vibrations in carbonyl groups is indicated by the signal at 1636.00 cm^{-1} . It is possible that the Al-O stretching vibrations of the Al_2O_3 nanoparticles correspond to the peaks at 460.17 cm^{-1} and 481.39 cm^{-1} .

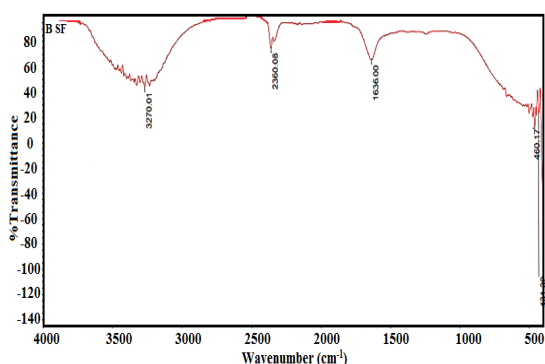


Fig. 3. FTIR Spectrum of Alumina NPs

Dynamic Light Scattering

The size distribution of alumina nanoparticles (Fig. 4), with an average size of 94.6nm and a PDI of 0.329 are shown in DLS. Lower PDI values indicate narrower size distributions. DLS data indicate a size distribution peak at 94.6nm, the average size of alumina nanoparticles. A higher PDI indicates a more polydisperse sample and a wider peak. With a PDI of 0.329, the particle size distribution is narrow, with a small variation around 94.6nm²⁷⁻²⁸.

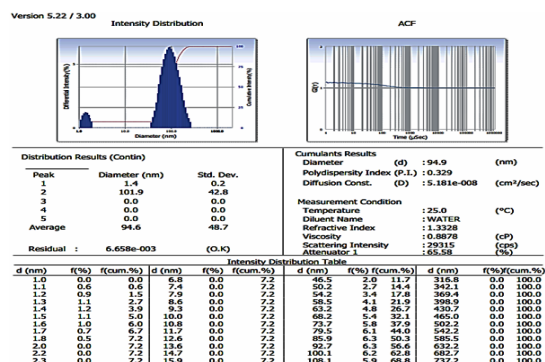


Fig. 4. Size distribution of alumina Nps

Morphology of Alumina NPs

SEM was utilized to characterize the morphology of the alumina nanoparticles, revealing

diverse shapes in scanning electron microscopy images. While most of the nanoparticles were spherical, some appeared elongated. The NPs' sizes showed some diversity (Fig. 5). Al_2O_3 NPs ranged in size from 1 μm to 100nm.

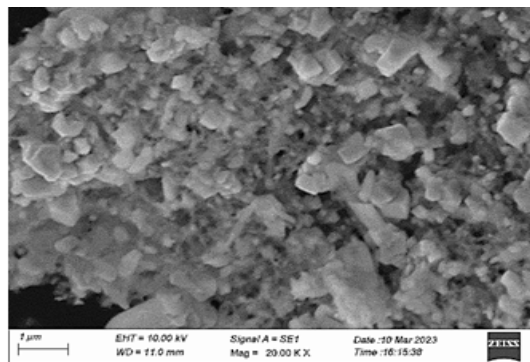


Fig. 5(a). SEM of Alumina NPs at 1µm

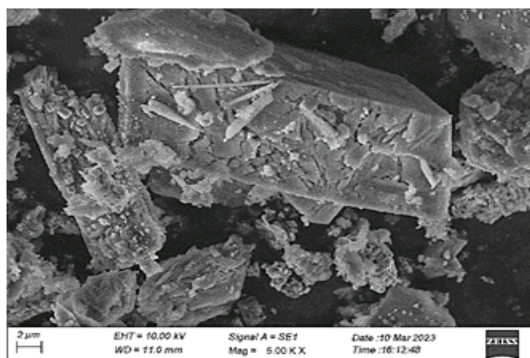


Fig. 5(b). SEM of Alumina NPs at 2µm

Fibre interaction was tested using SEM pictures. QUANTA 200 equipment with working distance 10.7 to 11.0mm and voltage 15 and 20kV was used for this investigation. Alumina nanoparticles made from leaf extract were studied for their shape. The nanoparticles had a spherical form and a size of 1 micrometre, which is quite tiny in the nanoscale range²⁹.

Crystalline study

Crystalline materials may be characterised non-destructively using X-ray diffraction (XRD). It reveals crystal structure, phase, texture, and key structural properties like grain size, crystallinity, strain, and defects. Peaks in XRD patterns arise from constructive X-ray interference, reflecting lattice atom distribution. XRD patterns estimated powders' average crystallite size using Scherrer's equation. XRD measured synthesised particle structure. Fig. 6 shows the XRD measurement for Al NP target

from *Solanum torvum* leaf extract. The sample had peaks at $2\theta^\circ = 28.81^\circ, 36.73^\circ, 43.68^\circ, 67.44^\circ, 71.36^\circ$ corresponding to lattice planes (104), (110), (012), (116), (214)³⁰.

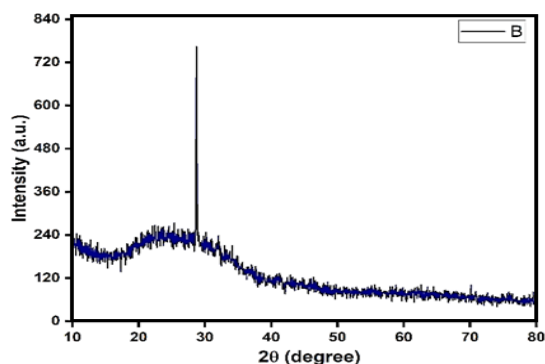


Fig. 6. XRD of Alumina nanoparticles

Antibacterial studies

Alumina nanoparticles (Al_2O_3 NPs) from plant extracts are commonly assessed for antibacterial activity using the well diffusion method. Bacteria cultured on agar plates with wells (Fig. 7) are exposed to the nanoparticle solution, and the resulting zone of inhibition indicates antibacterial effects. Antibacterial studies using the well diffusion method with Al_2O_3 NPs from plant extracts demonstrated inhibition of both *Gram-positive* and *Gram-negative* bacterial strains. Inhibition varied with nanoparticle concentration and bacterial strain. Nutritional agar plates were inoculated and dried before wells were created. Nanoparticle solutions (20 to 50 μL) were added to wells, and plates were incubated. Zones of inhibition around wells indicated bacterial or fungal growth suppression. Tuberculosis, a worldwide health issue, is caused by *Mycobacterium tuberculosis*. Dental caries is caused by *Streptococcus aureus*. Well diffusion test results are significant because these microorganisms are hard to treat. Plant extracts are used to synthesise antibacterial alumina NPs³¹. This work suggests that plant extract-derived alumina NPs may be a source of new antibacterial agents for TB and dental caries therapy. The control had a smaller zone of inhibition than *Mycobacterium tuberculosis* (24mm) and *Streptococcus mutans* (22mm). Al_2O_3 NPs synthesised from plant extract had a zone of inhibition of 18 to 24mm, indicating moderate to high antibacterial activity against *E. coli* *Gram-negative* bacteria. At 100 μL , Gentamicin

measured 20mm. *Candida albicans* showed considerable inhibition (12 to 18mm) compared to the control.

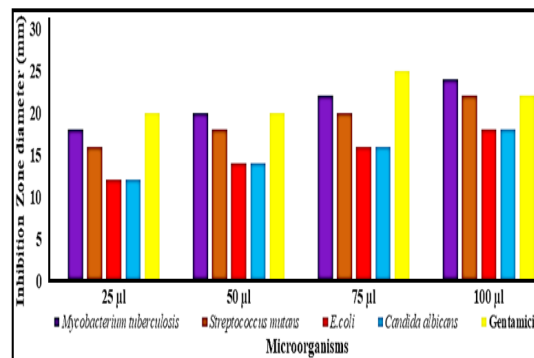


Fig. 7(a). Comparative analysis of Nps on bacterial strains

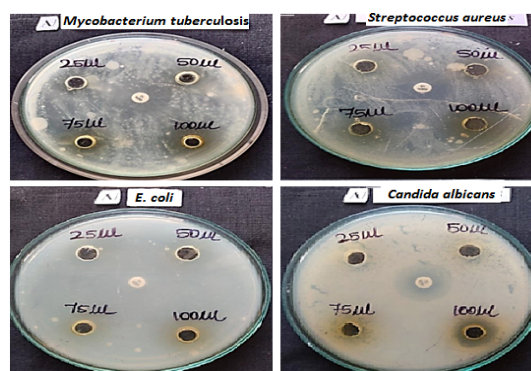


Fig. 7(b). Alumina NP inhibition zones

CONCLUSION

In conclusion, the study confirms that aluminum oxide nanoparticles (Al_2O_3 NPs) synthesized from *Solanum torvum* leaf extract provide an eco-friendly and cost-effective method for nanoparticle production. The comprehensive characterization of these nanoparticles demonstrates their high crystallinity and diverse morphologies, which are indicative of their structural integrity and stability. The significant antibacterial activity observed against multiple pathogens underscores the potential applications of these nanoparticles in healthcare and environmental sectors. The study highlights the advantages of using *Solanum torvum* leaf extract for green synthesis, emphasizing the broader implications for sustainable nanomaterial production. Future investigations could focus on optimizing synthesis parameters and exploring additional applications, further advancing the field of environmentally friendly nanotechnology.

ACKNOWLEDGMENT

"We extend our sincere gratitude to the Management of Nehru Memorial College (Autonomous) for their invaluable support, and to the dedicated M.Sc. students for their relentless efforts

in advancing our research. Also, we appreciate the unwavering support and encouragement from the Management of Dhanalakshmi Srinivasan University.

Conflict of interest

There is no conflict of interest.

REFERENCES

- Ahmad, S.; Munir, S.; Zeb, N.; Ullah, A.; Khan, B.; Ali, J.; Muhammad, B.; Omer, M.; Alamzeb, M.; Salman, S. M.; Ali, S., *Int. J. Nanomedicine.*, **2019**, *14*, 5087-5107. <https://doi.org/10.2147/IJN.S200254>.
- Ugo, J.; Nwamarah Raymond Ade, A.; Joy, A. T., *J. Food Nutr. Res.*, **2019**, *2*, 274-282. <https://doi.org/10.26502/jfsnr.2642-11000026>.
- Rotti, R. B.; Sunitha, D V.; Manjunath, R.; Roy, A.; Mayegowda, S B.; Gnanaprakash, A P.; Alghamdi, S.; Almeahadi, M.; Abdulaziz, O.; Allahyani, M.; Aljuaid, A.; Alsaiani, A A.; Ashgar, S. S.; Babalghith, A O.; Abd El-Lateef, A. E.; Khidir E. B., *Front. Chem.*, **2023**, *11*, 1143614. <http://doi: 10.3389/fchem.2023.1143614>.
- De, A.; Ghosh, S.; Chakrabarti, M.; Ghosh, I.; Banerjee, R.; Mukherjee, A., *Toxicol. Ind. Health.*, **2020**, *36*, 567-579. <http://doi: 10.1177/0748233720936828>.
- Igbokwe, I. O.; Igwenagu, E.; Igbokwe, N. A.; Interdiscip., *Toxicol.*, **2019**, *12*, 45. <http://doi: 10.2478/intox-2019-0007>.
- Ilavenil, K. K.; Kasthuri, A.; Pandian, P., *Rasayan J. Chem.*, **2023**, *16*, 596-603. <http://doi.org/10.31788/RJC.2023.1628221>.
- El-Kady, M. M.; Ansari, I.; Arora, C.; Rai, N.; Soni, S.; Verma, D. K.; Singh, P.; Mahmoud, A. E. D., *J. Mol. Liq.*, **2023**, *370*, 121046.
- El-Samad, L M.; El-Ashram, S.; Hussein, H. K.; Abdul-Aziz, K. K.; Radwan, E. H.; Bakr, N. R.; El Wakil, A.; Augustyniak, M., *Sci. Total Environ.*, **2022**, *806*, 150644. <https://doi.org/10.1016/j.scitotenv.2021.150644>.
- Yokel, R. A., *Crit. Rev. Toxicol.*, **2020**, *50*, 551-593. <https://doi.org/10.1080/10408444.2020.1801575>.
- Mounesh, K.; Yatish, V.; Pandith Anup, E. G. E., *J. Mater. Chem. B.*, **2023**, *11*, 10692-10705.
- Ghosh, S.; Ahmad, R.; Zeyaulah, M.; Khare, S. K., *Front. Chem.*, **2021**, *9*, 626834. <http://doi.org/10.3389/fchem.2021.626834>.
- Ibrahim, E.; Zhang, M.; Zhang, Y.; Hossain, A.; Qiu, W.; Chen, Y.; Wang, Y.; Wu, W.; Sun, G.; Li, B., *Nanomaterials.*, **2020**, *10*, 219. <https://doi.org/10.3390/nano10020219>.
- Ghotekar, S., *Nanochem. Res.*, **2019**, *4*, 163-169. <https://doi.org/10.22036/ncr.2019.02.008>.
- Rizwana, H.; Bokahri, N. A.; Alkhattaf, F. S.; Albasher, G.; Aldehaish, H. A., *Molecules.*, **2021**, *26*, 7709. <https://doi.org/10.3390/molecules26247709>.
- Manikandan, V.; Jayanthi, P.; Priyadharsan, A.; Vijayaprathap, E.; Anbarasan, P. M.; Velmurugan, P., *J. Photochem. Photobiol. A Chem.*, **2019**, *371*, 205-215. <https://doi.org/10.1016/j.jphotochem.2018.11.009>.
- Goutam, S. P.; Avinashi, S. K.; Yadav, M.; Roy, D.; Shastri, R., *Adv. Sci. Eng. Med.*, **2018**, *10*, 719-722. <https://doi.org/10.1166/ase.2018.2236>.
- Koopi, H.; Buazar, F., *Ceram. Int.*, **2018**, *44*, 8940-8945.
- Ragavendran, C.; Kamaraj, C.; Alrefaei, A. F.; Priyadharsan, A.; de Matos L. P.; Malafaia, G.; Moulishankar, A.; Thirugnanasambandam S. S., *Afr. J. Bot.*, **2024**, *167*, 643-662. <https://doi.org/10.1016/j.sajb.2024.02.049>.
- Pugazhendhi, S.; Jayavel, R., *Inorg. Chem. Commun.*, **2023**, *156*, 111129. <https://doi.org/10.1016/j.inoche.2023.111129>.
- Renuka, R. K.; Renuka, D.; Sivakami, M.; Thilagavathi, T., *J. Plant Biochem. Biotechnol.*, **2021**, *3*, 596-601. <https://doi.org/10.1007/s13562-021-00650-8>.
- Narayanan, M. V.; Rakesh, S., *IOP Conf. Ser. Mater. Sci. Eng.*, **2018**, *402*(1), 012150. <https://doi.org/10.1088/1757-899X/402/1/012150>.
- Sharma, P.; Sharma, N., *Int. J. Eng. Appl. Sci. Technol.*, **2020**, *5*, 251-253.

23. Hassanpour, P.; Panahi, Y.; Ebrahimi-Kalan, A.; Akbarzadeh, A.; Davaran, S.; Nasibova, A. N.; Khalilov, R.; Kavetsky, T., *Micro Nano Lett.*, **2018**, *13*, 1227-1231. <https://doi.org/10.1049/mnl.2018.5070>.
24. Farahmandjou, M.; Golabiyan, N., *Int. J. Bio-Inorg. Hybr. Nanomater.*, **2016**, *5*, 73-77.
25. Duraisamy, P., *Int. J. Res. Appl. Sci. Eng. Technol.*, **2018**, *6*, 428-433.
26. Elumalai, E. K.; Prasad, T N V K V.; Venkata, K.; Nagajyothi, P. C.; David, E., *Arch. Appl. Sci. Res.*, **2010**, *2*, 76-81.
27. Kumar, A.; Behl, T.; Chadha, S., *Int. J. Biol. Macromol.*, **2020**, *149*, 1262-1274. <https://doi.org/10.1016/j.ijbiomac.2020.02.048>.
28. Karthik, C.; Suresh, S.; Sneha Mirulalini, G.; Kavitha, S., *Inorg. Nano-Met. Chem.*, **2020**, *50*, 606-612.
29. Sumesh, K. R.; Kanthavel, K.; Vivek, S., *Mater. Res. Express.*, **2019**, *6*, <https://doi.org/10.1088/2053-1591/aaff1a>.
30. Liu, C.; Zhang, A. J.; He, B. Y.; Wang, A. P., *Aust. J. Chem.*, **2017**, *70*, 120-204.
31. Manogar, P.; Morvinyabesh, J. E.; Ramesh, P.; Jeyaleela, G. D.; Amalan, V.; Ajarem, J. S.; Allam, A. A.; Khim, J. S.; Vijayakumar, N., *Materials Letters.*, **2022**, *311*, 131569. <https://doi.org/10.1016/j.matlet.2021.131569>.